

## Sea state bias in satellite altimetry: models rating, limitations and optimal parameters

Roman E. Glazman, Alexander Greysukh and Victor Zlotnicki

Jet Propulsion laboratory, California Institute of Technology, Pasadena, CA 91109.  
U.S.A.

### ABSTRACT

Investigations of the sea state bias in altimeter measurements of sea surface height have been reported by many authors based on aircraft, sea tower and satellite borne observations, resulting in several proposed algorithms of the form  $SSB = \epsilon H$  where  $H$  is the significant wave height (SWH) and  $\epsilon$  is a nondimensional function of wind and wave parameters. The reported values for empirical coefficients in these algorithms differ widely. In the present work, based on the most complete set of satellite measurements (Geosat altimeter) employed for such studies, all known algorithms are rated. The most popular, linear Geophysical Model Function (GMF), of the form  $\epsilon = a_0 + a_1 U$ , is shown to yield an improvement over the simplest GMF with a constant  $c$ . A three-parameter linear form  $\epsilon = a_0 + a_1 U + a_2 H$  produces even better results. However, the accuracy of the polynomial models is below that obtained with a two-parameter, physically-based GMF relating  $\epsilon$  to the pseudo-wave-age  $\xi$ :  $\epsilon = M \xi^{-m}$ . The  $\xi$  is estimated using altimeter wind  $U$  and SWH:  $\xi \approx A(gH/U)^v$  where  $A$  and  $v$  are constants. All models are tested on global data as well as on a few selected regional data sets. For all SSB models, empirical parameters yielding best results for global data sets produce poor results for certain regions. By analyzing performance and parameters of different models we conclude that further progress can hardly be achieved by raising the degree of the polynomial for  $\epsilon(U, H)$ . Physically-based approaches employing a small number of adjustable parameters and theoretically justified non-dimensional combinations of external wind and wave factors appear to be more promising.

Submitted to Journ. Geophys. Res., Oceans. April 1993

## 1. Introduction

The accuracy of range measurements by present satellite altimeters onboard IRS-1 and Topex is about 2 cm - in terms of the distance between the satellite antenna and the apparent mean sea level. For Topex, the accuracy of satellite orbit determination is better than 10 cm (in terms of the altitude), which is achieved due to the use of the laser and Doppler (DORIS) satellite tracking, as well as due to the low drag on the satellite flying at the 1336 km altitude and recent improvements in gravity field models. Jbus, the task of accounting for the sea state bias (SSB) - which may well exceed 10 cm - moves to the forefront. SSB is the difference between the apparent mean sea level - as "seen" by an altimeter - and the true mean sea level - defined as the mean height found by averaging the surface elevation field over the footprint area. The SSB correction, according to theoretical prediction [Glazman and Srokosz, 1991] varies between 1 and 20 cm - depending on the significant wave height ( $S_{WJ1}$ ), wave age and other factors. Experimental data indicate that this prediction is reasonable.

While a number of algorithms for the SSB correction have been proposed in recent years, their actual performance under realistic ocean conditions has not been tested. More importantly, there is considerable disagreement in the literature as to the functions] form in which SSB is to be sought. Most of the contemporary models assume SSB to be linear] y proportional to  $S_{WJ1}$ . Jhc proportionality coefficient,  $c$ , (introduced by equation (1)) is (almost linearly) related to the local wind. An exception is given by a physically-based model [Glazman and Srokosz, 1991; Fu and Glazman, 1991] which indicates that, for global data, the SSB dependence on  $S_{WJ1}$  is weaker: at a given wind, SSB is approximately proportional to the square root of SWH, although the wind speed dependence of the proportionality coefficient remains close to linear. The theory suggests that SSB is controlled primarily by the degree of the sea development which can be crudely quantified by two non-dimensional parameters - the wave age and the ratio of the wind fetch to the intrinsic inner scale of the gravity wave turbulence. Practical implementation of this model requires expressing these factors in terms of the satellite-reported quantities - wind speed and SWH, which is not always possible. Jbus, the central issue addressed by the present work is the form in which the SSB correction should be sought and limitations of the present paradigm.

A 2.5 year set of global Geosat altimeter measurements, as described in section 4, is employed. This data set allowed us to create a large number of subsets - both with global and regional coverage. In sections 4 and 5 the data preparation and analysis procedures are described in detail. One of our main conclusions, section 7, is that none of the

presently available empirical model functions is capable of providing uniformly valid SSB estimates: the SSB models tuned on global data yield poor results for certain ocean regions. Possible causes of such inconsistencies are discussed in sections 6 and 7.

The values of SS11 model parameters determined by Fu and Glazman exhibited large scatter (among individual satellite passes) which made it difficult to select best values for global applications. Moreover, those parameters (as well as the parameters of other SSB models) were affected by a wave-age-related error trend in the altimeter wind speed algorithm (the Brown algorithm). Since SSB itself is a function of the wave age, the Brown algorithm imported ambiguity into the SSB model. Recently [Glazman and Greysukh, 1993], new wind speed algorithms were developed in which the wave-age-related error trend is reduced to a geophysically-insignificant level. Here we shall use the algorithm that uses a smooth classifier as described in section 6 of that paper. This model function allows one to obtain unbiased parameters for SSB models and reduces the scatter in the values of these parameters. The refined model parameters for all SSB algorithms are reported in section 5.

According to the presently accepted terminology, SSB is the total error in sea level measurements caused by various effects of sea surface roughness. It includes two components: one due to distortion of the reflected pulse shape ("wave form") and another one due to a shift (delay) of the entire pulse as a whole. The first component is linearly proportional to the sea surface skewness,  $\langle \zeta^3 \rangle / \langle \zeta^2 \rangle^{3/2}$ , where  $\zeta$  is the surface height affected by wind-generated waves, and the second represents the difference between the mean ("true") sea surface height and the mean height of the specular facets of an undulating water surface. These facets produce reflection of the incident radar signal back to the satellite. The difference is often referred to as the IM bias (for electromagnetic). In the present work we investigate the total error, i.e., SSB. The theory of sea level measurements is described, e.g., by Brown [1977], Hayne [1980], Barrick and Lipa [1985], Rodriguez [1988] and Glazman and Srokosz [1991]. The latter work focuses on effects of open ocean waves emphasizing sea wave dynamics and statistics. Relationships expressing SSB as a function of sea state parameters are briefly reviewed in the next section and a few comments regarding the interpretation of experimental results are also suggested. A statistical technique employed to estimate empirical parameters in the models is presented in section 3, and the corresponding calculations are reported in section 5. In section 6, we rate different SS13 models according to their accuracy and offer recommendations for future work.

## 2. Sea state bias and its geophysical model function

The SSB is usually sought in the form

$$\eta = \epsilon H \quad (1)$$

where  $\epsilon$  is a **non-dimensional** coefficient varying from 0.01 to 0.06- as follows from a large number of studies (reviewed by Walsh et al. [ 1989], Chelton et al. [ 1989] and Melville et al. [ 1991]), and  $H$  is the significant wave height (usually denoted as  $H_{1/3}$ ). This form has a theoretical basis [Jackson, 1979], [Glazman and Srokosz, 1991]. The theory also predicts that  $\epsilon$ , which accounts for both the distortion of the return pulse shape and the delay in the pulse return, is a function of the wave age  $\xi$  and of the ratio of the intrinsic surface microscale,  $h$ , to the wind fetch,  $X$ .

$$\epsilon = F(\xi, h/X) , \quad (2)$$

where

$$\xi = C_0/U \quad (3)$$

$U$  is the mean wind above the sea surface,  $C_0$  is the phase velocity of the dominant (spectra] peak) waves. Parameter  $h$  has been introduced earlier [Glazman, 1986]. Its estimate for developed seas [Glazman and Weichman, 1989] is about 0.5 m. Under additional assumptions, detailed in section 8 of [Glazman and Srokosz, 1991], the dependence of  $\epsilon$  on  $h/X$  can be foregone: implying that  $h/X$  in (2) can be replaced by a constant (understood as the average  $\langle h/X \rangle$  representative of the global data set) one is left with  $\epsilon \approx F(\xi)$ . Since the actual wind fetch is usually unknown (and poorly defined), this simplification is of great practical value. Specifically, the SSB coefficient  $\epsilon$  can be approximated by

$$\epsilon \approx M\xi^{-m}, \quad (4)$$

where  $M$  and  $m$  are constants [Glazman and Srokosz, 1991], [Fu and Glazman, 1991]. Relationship (4) is highly useful because, under idealized sea conditions,  $\xi$  can be estimated given the mean wind and the significant wave height [Glazman et al, 1988] from altimeter measurements:

$$\xi \approx A(gH/U^2)^v \quad (5)$$

Parameters  $A$  and  $v$  have been determined theoretically [Glazman and Srokosz, 1991; Glazman, 1993] as well as experimentally [Glazman and Pilorz, 1990; Glazman, 1993]:  $A \approx 3.21$ ,  $v \approx 0.31$ . When the sea conditions are more complicated than those required for a rigorous justification of (5), the latter should be viewed as an *ad hoc* function whose relevance is to be tested by observations. Equation (5) then provides a measure of

sea development which should be appropriately called the “pseudo wave age” [Fu and Glazman, 1991]. Based on large amounts of data, this quantity has been shown to be practically useful, and radar return has been found to depend on  $\xi$  in a fashion consistent with the theoretical predictions [Glazman and Pilorz, 1990].

Aircraft and tower-based radar experiments have suggested that, for a given radar frequency,  $\epsilon$  can be sought as a function of  $U$  [Choy et al., 1984], [Walsh et al., 1984, 1991] or of  $U$  and  $H^{1/3}$  [Melville et al., 1991]. The corresponding empirical relationships have been sought in the form:

$$\epsilon = a_0 + a_1 U + a_2 H \quad (6)$$

Since  $U$  is usually estimated based on the radar cross section  $\sigma_0$ , an alternative form

$$\epsilon = a_0 + a_1 \sigma_0^2 + a_2 H \quad (7)$$

has also been proposed [Melville et al., 1991]. Relationship (6) with  $a_2=0$  is supported by actual satellite data - as reported by Ray and Koblinsky [1991]. Empirical coefficients  $a_n$  reported by different authors are summarized in Table 1.

Of course, equations (6) and (7) are physically meaningless, unless parameters  $a_n$  can be interpreted in terms of appropriate dimensional quantities. It turns out that such a physically-based interpretation is possible, for example - by using (4) and (5). Apparently, one can approximate (4) and (5) by

$$\epsilon = F(U, H) \approx c_0 + c_1 U + c_2 H + c_3 UH + c_4 U^2 + c_5 H^2 + \dots \quad (8)$$

where dimensional coefficients  $c_n$  can be found from a Taylor series expansion of  $F(\xi(U, H))$  about some (mean) values of  $U$  and  $H$ . Such an exercise would immediately demonstrate that: (i) equation (6) must include additional terms in order to parametrize the dependence of  $\epsilon$  on sea conditions for a sufficiently wide range of sea states, and (ii) the coefficients of expansion, being functions of the mean  $U$  and  $H$ , depend on the choice of these mean values. Therefore, when determined empirically, the coefficients all in the GMFs (6) and (8) will differ among different investigators, unless such a determination is based on a global data set representing a statistically faithful sample of all possible sea states.

Practically, encumbering equation (6) with additional terms would greatly complicate the task of empirical “tuning” all these coefficients. Even the simplest, linear, form of (8) - as presented by (6) - contains a greater number of adjustable coefficients than does the physically-based model (4). Therefore, the most practical approach to the problem is to

use the theoretical relationships (4)-(5) directly and determine parameters  $M$  and  $M$  which provide the best fit to the global data, in section 5, functions of type (6) and (7) are shown to be less advantageous for representing observed global trends, although they may yield useful approximations for special situations and/or local conditions.

Finally, let us clarify a few important points regarding the interpretation of aircraft and tower-based observations. The physical cause of SSB, as understood by most experimentalists, appears to be somewhat different from that accepted in theoretical literature. However, the two views can be reconciled in a special case of a poorly developed sea. Experimentalists, especially those working with narrow-beam radars at small altitude [Yaplee et al., 1971; Choy et al., 1984; Walsh et al., 1984,1989,1991; Melville et al., 1991], record time history of the radar power returning from a small illuminated spot (under 2 meter in diameter) of an undulating sea surface. Dependence of the return power on the position  $\mathbf{x}_i$  of the spot with respect to the phase of the dominant water wave is of main interest in such studies: greater reflection from wave troughs in comparison to that from wave crests is related to the electromagnetic bias in altimeter measurements. Practically, the em. bias can be estimated as

$$h = \frac{\sum \zeta(\mathbf{x}_i) \sigma_0(\mathbf{x}_i)}{\sum \sigma_0(\mathbf{x}_i)}, \quad (9)$$

where  $\sigma_0(\mathbf{x}_i)$  is the power returned from a spot centered at  $\mathbf{x}_i$  and summation (over  $i$ ) covers a sea surface patch enclosing many dominant wave lengths [Melville et al., 1991].

According to theory based on geometrical optics, radar backscatter comes from small surface facets oriented perpendicular to the radar beam. Hence, "brighter" wave troughs and "darker" wave crests mean that a large number of smaller-scale ripples having specular facets are distributed over the large-scale, i.e. dominant, wave shape in a highly non-uniformly fashion: these ripples are rare near the crests of dominant waves and numerous near the troughs. In a sea characterized by a narrow-band wave spectrum, the crests of large-scale-waves are of course above the mean sea level and the wave troughs are below. It is then natural to expect that (9) will produce a reasonable estimate of the sea state bias. However, in a developed sea characterized by a continuous hierarchy of surface wavelets of all sizes, many of the wave troughs are found above the mean sea level and many wave crests below, and the very notion of wave crests and troughs becomes meaningless [Glazman and Weichman, 1989]. Results based on (9) will be unacceptably sensitive to the size of the radar footprint and to the electromagnetic frequency: the latter determines the characteristic size of the sea surface areas playing the

role of individual specular reflectors. This is why the results of “sea state bias” measurements using narrow-beam, low-altitude radars are difficult to extrapolate to the case of satellite altimeter observations. This conclusion is confirmed by the analysis presented in sections 5 and 6.

### 3. Determination of SSB based on satellite altimeter data

While tower-based and aircraft measurements in principle allow comparison between the altimeter-reported sea surface height and the true mean sea level, global measurements by a satellite altimeter cannot be checked by *in situ* observations. Determination of SSB then has to be carried out by examining variations in the altimeter-reported sea level and extracting a component that is due exclusively to variations of sea surface roughness associated with wind-generated waves. A technique that has proved highly successful was probably first used for this task by Born et al. [1982]. More recently, modifications of this technique were used by Zlotnicki et al. [1989], Ray and Koblinsky [1991] and Fu and Glazman [1991]. The same basic approach is implemented in the present work: we seek an optimal dependence of SSB on wind-wave characteristics by minimizing the total variance  $\langle(\Delta\zeta)^2\rangle$  of all sea level increments calculated for geographic points of interest. In contrast to the previous work, we shall use large sets of points uniformly covering an ocean area, i.e., sampled from many satellite passes. This will allow us to better understand variability of the model parameters as functions of environmental conditions. Ultimately, we shall determine the optimal parameters for global applications.

Let the altimeter-reported sea surface height at a horizontal position  $i$  and time  $n$  be the sum of the true height,  $\zeta_i^{\text{true}}$ , the uncertainties in the geoid, satellite orbit and similar factors unrelated to sea surface roughness and denoted summarily as  $h_i$ , and the SSB denoted as  $\eta_i$ :

$$\zeta_i(n) = \zeta_i^{\text{true}}(n) + h_i(n) + \eta_i(n) \quad (10)$$

The total variance sought is the average of all temporal increments squared over all time steps for each point  $i$  (and then over all points):

$$\langle(\Delta\zeta)^2\rangle = (1/N)\sum (\zeta_i(n) - \zeta_i(k))^2 \quad (11)$$

where summation is done with respect to  $i, k$  and  $n$  ( $n \neq k$ ). For each point  $i$ , the total number  $J$  of increments is  $K(K-1)/2$  where  $K$  is the number of sea surface height measurements made at that point during altimeter observations. Finally, the total number  $N$  of terms in (11) is  $J \cdot I$  where  $I$  is the number of points for which altimeter data have been used. Assuming that neither  $\zeta_i^{\text{true}}$  nor  $h_i$  are correlated with  $\eta_i$ , equation (11) can be simplified by setting the mean of all products  $(\Delta\zeta_i^{\text{true}}\Delta\eta_i)$  and  $(Ah_i\Delta\eta_i)$  to zero. Moreover, one can also assume  $\zeta_i^{\text{true}}$  and  $h_i$  to be uncorrelated, although this assumption is not critical for the success of the approach. Let us denote the averaging operation by  $\langle \rangle$  and write the end result as:

$$\langle (\Delta\zeta)^2 \rangle = \langle (\Delta Z)^2 \rangle + \langle (\Delta\eta)^2 \rangle \quad (12)$$

where  $\Delta Z = [\zeta_i^{\text{true}}(n) + h_i(n)] - [\zeta_i^{\text{true}}(k) + h_i(k)]$ . One particular advantage of this approach is that all time-invariant components (such as the geoid uncertainty) of the total error in sea surface height are canceled. Nevertheless, the contribution of  $\langle (\Delta\eta)^2 \rangle$  to  $\langle (\Delta\zeta)^2 \rangle$  is much smaller than that of  $\langle (\Delta Z)^2 \rangle$ , for the sea level variability is dominated by surface oscillations associated with ocean circulation, tides, mesoscale eddies, etc., rather than by effects of wind-generated surface gravity waves.

Increments  $\Delta\eta$  are expressed in terms of wind-wave parameters:

$$\Delta\eta = c(n)\eta(n) - \epsilon(k)\eta(k), \quad (13)$$

where subscript  $i$  is omitted for brevity. The use of (1)-(4) yields:

$$\Delta\eta = M[\xi^{-m}(n)\eta(n) - \xi^{-m}(k)\eta(k)], \quad (14)$$

Empirical values of  $M$  and  $m$  are found by minimizing  $\langle (\Delta\zeta)^2 \rangle$  as a function of these parameters. In Fig. 1 we illustrate this function for a case of global observations. Other forms of  $\eta_i$ , in particular those based on (6), (7) or (8), can be used as well, in which case the parameters to be optimized are  $a_n$  or  $c_n$ , respectively.

As discussed in the next section, in place of the sea surface height  $\zeta$ , we actually use the deviations of the measured height from the height obtained by averaging at a given point of all the observations over the entire period. However, it is easy to show that



relationships (12) and (13) remain just as valid for these deviations as they are for the real heights  $\zeta_i(n)$ .

#### 4. Geosat data employed

The NOAA/National Ocean Survey Geophysical Data Record CD-ROMS (Cheney et al., 1991) were used. They differ from the older version of the Geosat data (Cheney et al., 1987) by the use of a more accurate GEM-T2 orbit (Laines et al., 1990), water vapor corrections derived from TOVS data (Fimery et al., 1990) prior to July 1987 and from SSM/I data (Wentz, 1989) after that date, and the correction of software errors in the computation of Schwiderski's tidal model (Cheney, 1991, pers. comm.). These data were edited for blunders, regridded to a uniform set of alongtrack latitudes (Zlotnicki et al., 1990), and differenced from the most complete track (see Zlotnicki, 1991 for a summary of the method). Residual orbit error was removed as described below. Finally, the sea surface height residuals from the 1987-88 mean sea level were generated - because the geoid is not known to sufficient accuracy at this time.

The GEM-T2 orbit, like its predecessors, is the result of a dynamically consistent computation, where the satellite's orbital parameters are adjusted to the tracking data (Doppler in the case of Geosat) but are constrained to obey the equations of motion of the satellite subject to (imperfect) models of the forces (gravity, drag, solar pressure, etc) acting on the satellite. The GEM-T2 orbit computation leaves a 30 cm rms residual orbit error: 17.0 cm in 1987 and 40.1 cm rms in 1988, due to increased solar activity in the second half of 1988, which increases insufficiently modeled drag forces on the satellite. These values were reduced by fitting and removing a once per revolution sine function fitted over a complete period of the satellite (approximately 6037.5 sec or 40,030 km alongtrack). After orbit error removal, the mean sea level at each latitude-longitude point over 1987-88 was computed and removed from the time series for that point. Blunders were presumed whenever sea level residuals exceed five times the rms of the data either alongtrack (fixed time within 100 min) or at fixed latitude-longitude; such blunders were removed, the residual orbit correction was recomputed and the process iterated up to four times, or fewer if no more blunders were detected.

The final product of these steps are sea level residuals from a 2.5 year mean, approximately every 7 km alongtrack, repeated once every 17.05 days along each track, with parallel neighboring tracks occurring some 164 km (at the equator) and 3.0 days later to the east, plus another set of parallel tracks in the other (ascending or descending) direction.

in order to reduce adverse influence of “bad” measurements, we eliminated cases with excessively large satellite attitude angles (i.e., when the off-nadir pointing angle exceeded 0.82 degree which was found earlier [Glazman and Pilorz, 1990] to distort  $\sigma_0$  and SWH). Also eliminated arc cases with  $\sigma_0 < 6$  dB and  $\sigma_0 > 25$  dB, and SWH  $< 0.1$  m. Furthermore, a nine-point median filter was applied to the sea level, SWH and  $\sigma_0$  - in order to reduce measurement noise and to be able to compare the present results with those of the previous work [Fu and Glazman, 1991]. Possible influence of this filtering on the results is discussed in section 6. Finally, these three parameters were subsampled every third point along the tracks.

### S. Experimental procedure

In this section we provide a detailed description of “experiments” carried out in this work, while the interpretation of the results is given in section 6.

Besides rating various SSB algorithms, we want to assess the variability of the sea state bias and its sensitivity to wind speed and wave age under different types of environmental conditions. Ultimately we need to derive statistically significant values of optimal model parameters for global applications. Therefore, our present use of satellite data is rather different from that described by Fu and Glazman [1991] and by other authors. Employing data separately for each individual satellite track, FG obtained 16 sets of model parameters - corresponding to the number of orbits used. These were then averaged to obtain model parameters appropriate for global applications. Unfortunately, those 16 orbits did not provide a uniform global coverage, hence the question of their representativeness with respect to global data remained open. In the present work, we subset the data not by the orbits but by the regions which include all relevant satellite orbits. One of the regions is the entire ocean, for which we assembled 20 global data subsets composed of 163 points each, providing uniform global coverage. These points generated up to 55,000 pairs of  $\zeta_i$  to form sea level differences. For each region under study (shown in Fig. 2), including global subsets, we estimated the optimal model parameters, the mean wind, mean SWH, mean pseudo wave age  $\xi$ , mean “generalized wind fetch” (15), and the  $\langle (\Delta\zeta)^2 \rangle^{1/2}$  before and after the SSB correction. Most of these parameters are summarized in Table 2. The last row gives the mean values for the global subsets.

Selecting the regions shown in Fig. 2 we tried to cover most diverse conditions to see if variations in the SSB behavior are related to regional anomalies. For instance, regions 1 and 4 are characterized by a relatively small variability of the mean sea level - reflecting a low level of mesoscale dynamic activity. Regions 7 and 8 have much higher

activity in terms of total  $\langle(\Delta\zeta)^2\rangle^{1/2}$ . Regions 2 and 8 are characterized by relatively poorly developed seas - as reflected in the low values of both pseudo wave age  $\xi$  and pseudo wind fetch  $X$ , whereas regions 1,3, 6 and 7 represent mature seas. In Figure 3 we show regional variation in the behavior of the SSB coefficient  $\epsilon(\xi)$ . This plot is based on representing  $\epsilon(\xi)$  in the form  $b_1\xi + b_2\xi^2$  for which parameters were determined as optimal coefficients for individual regions. This flexible form does not constrain  $\epsilon(\xi)$  to a particular behavior such as, for instance, a power law (4). The reader is also invited to plot an analogous set of curves for a linear wind algorithm by employing the coefficients  $a_0$  and  $a_1$  provided in Table 2. Such plots illustrate the great diversity of wind-wave interaction conditions characterizing individual ocean regions, and are further discussed in the next section.

The statistically significant optimal model parameters for global applications were obtained as averages over the 20 global subsets. To test these parameters and to compare the global SSB model to the other models, we ultimately created three independent subsets of global data, each composed of up to 400 points which had not been used in the derivation of the model parameters. For these three subsets we estimated  $\langle(\Delta\eta)^2\rangle^{1/2}$  for all algorithms under consideration. For each SSB model, variations in the values of  $\langle(\Delta\eta)^2\rangle^{1/2}$  among the test subsets were insignificant.

The only quantitative measure of improvement of altimeter measurements which can be assessed based on satellite data alone is the mean squared decrement  $\langle(\Delta\eta)^2\rangle$  by which the total sea level variance  $\langle(\Delta\zeta)^2\rangle$  is reduced owing to the SSB correction: the greater this decrement, the better the model performance. The square root of this quantity, called here the "accuracy gain," is reported in Table 1 for all algorithms tested including the optimized algorithms based on (6). It has been obtained as the average over the three test subsets.

The "generalized wind fetch"  $X$ , defined as

$$X = \frac{g(H/U)^2}{U^3} \quad (15)$$

[Glazman, 1987; Glazman and Pilonz, 1990], characterizes the ratio of the wave energy density (per unit surface area) to the mean wind kinetic energy density (per unit volume) and, under special conditions, is linearly proportional to the conventional geometric fetch. This quantity, estimated based on altimeter measurements of  $U$  and  $H$ , is provided in Table 2 and is discussed in the next section.

Equation (4) was employed by FG in the form  $\epsilon \approx A(\xi/\bar{\xi})^{-m}$  where  $\bar{\xi}$  is the mean pseudo-wave-age. In the present work we are using the form (4) directly. Since  $M = A\bar{\xi}^m$  and  $\bar{\xi}$  is known, these two forms are equivalent, and in Table 1 we provide

and  $M$  based on both the FG estimate and the present work. The scatter of  $m$  and  $M$  values among the 20 global subsets is illustrated in Figure 4. Comparing this plot with the results reported by FG for 16 satellite orbits one finds a significant decrease in the scatter of the experimental values of  $m$  and  $M$ . We are inclined to attribute this improvement to two factors: the present use of statistically similar global subsets and the present use of a more accurate wind speed algorithm [Glazman and Greysukh, 1993].

The minimization of  $\langle(\Delta\zeta)^2\rangle$  as a function of  $a_0, a_1$  and  $a_2$  in (6) or of  $m$  and  $M$  in (4) was carried out using a quasi-Newton method and a finite-difference gradient [Dennis and Schnabel, 1983]. This method is implemented in the IMSL routine DUMINF. Along with the derivation of the optimal model parameters, we found it instructive to plot  $\langle(\Delta\zeta)^2\rangle$ , as shown in figures 1, 5, 6 and 7. Indeed, the presence of a well defined minimum of this function, as found in Figure 1, confirms that a given SSB model is robust and its optimal parameters can be established unambiguously. If the minimum is difficult to identify, as is the case of Figures 6 and 7, the model is less reliable.

A SSB model can be declared successful only if it reduces the total variance of sea level increments by an amount exceeding that resulting from the simplest standard model  $SSB = a_0 \cdot H$ . Therefore, we also estimated the optimal constant  $\epsilon = a_0$  for each data subset and the corresponding accuracy gain  $\langle(\Delta\eta)^2\rangle$ , reported in Tables 1 and 2.

## 6. Analysis of the results

### 1. Existing SSB models

Comparing the accuracy gains in the last column of Table 1, we find that the best performance among all existing SSB models is achieved by the wave-agg-based model (4)-(5). All three algorithms A, B and C proposed by Melville et al. - equations (6) and (7) with the coefficients listed in Table 1 - lead to an increase rather than a decrease in the total variance of surface height increments  $\langle(\Delta\zeta)^2\rangle$ . The GMF proposed by Walsh et al. [1991] does improve the accuracy of sea level measurements in comparison to that without any SSB correction. However, the improvement is marginal. A better result is achieved by the Ray-Koblinsky model, probably because the model parameters have been tuned based on global satellite observations. However, the accuracy gain is still below that obtained with a constant  $c$ .

The accuracy gain of 1.9 cm corresponding to  $\epsilon = a_0 = 0.018$  can be viewed as the benchmark to be surpassed by any practically useful algorithm. It is difficult at the present time to indicate the maximum accuracy gain that would be achieved by the "perfect" algorithm, although it is clear that the 2.5 cm achieved by two models - (4) and

(6) - is not the limit to the improvement. The fact that the optimized model parameters,  $M=-0.026$  and  $m=0.56$ , found in the present work for equation (4) have not yielded an appreciable increase of the global accuracy (with respect to the accuracy gain obtained using the Fu and Glazman parameters) indicates that model (4) is robust and can be recommended for global applications.

## 2. Critique of polynomial models,

Comparing the three linear models based on (6) and analyzed in "Table 1, one finds that even the most complete, three-parameter, version of (6) is less accurate than the two-parameter model (4). Remembering the comments made in section 2, this conclusion is not unexpected. Moreover, the experiments reported in 'Table 1 confirm that expressions like (6) represent a crude approximation to a physically-based relationship (4). Indeed, the negative values of  $a_2$  appearing in Table 1 can be obtained by expanding (4),(5) in powers of  $(1 - \langle I \rangle)$ . One might try to obtain a better approximation by including higher-order terms - as shown in (8). However, such an approach is unlikely to succeed: each additional term requires an additional empirical parameter whose determination represents a formidable problem. Figures 5-7 give a taste of the difficulties to be expected here. We believe that more progress can be achieved by using physically-based models which would more fully account for the factors of sea surface's statistical geometry, for instance the theoretical model (2) illustrated in Figure 8 of [Glazman and Srokosz, 1991].

## 3. Regional studies as an indicator of additional factors of the sea state bias.

Zlotnicki et al [1989] found that the SSB coefficient,  $c$ , for the simplest model  $\epsilon = a_0$  differs appreciably among individual regions. In Table 2 we provide regional values of  $a_0$  for this model, as well as the values of  $a_0$  and  $a_1$  for the model (6) with  $a_2 = 0$ . Evidently, all these coefficients exhibit considerable variability, and the influence of the characteristic wind speed (which varies from region to region) on  $\epsilon$  cannot explain the regional variations of  $a_0$  and of other coefficients. Based on the findings of Witter and Chelton [1991] who reported the effect of "saturation" in the values of SSB at high SWH, one might expect that the regional variations of  $a_0$  (or of  $a_0$  and  $a_1$  in a wind-dependent model) are correlated with regional SWH. Figure 8a based on the data of Table 2 illustrates this dependence for  $\epsilon = a_0$ . Evidently, at high SWH,  $\epsilon$  dots tend to be small, although one experimental point (the Arabian Sea) provides a counter example. Figure 8b shows the dependence of  $\epsilon$  on  $X$ . Similarly to Fig. 8a, the SSB coefficient  $\epsilon$  is small at extremely high values of  $X$  (points 6 and 7). Moreover, curves 6 and 7 in Fig. 3 exhibit an exceptionally weak dependence on  $\xi$  thus confirming the "saturation effect." However, points 2, 3 and 8 in Fig. 8b challenge his simple model. Other external factors

summarized in Table 2, including the total sea level variance  $\langle (\Delta\zeta)^2 \rangle$ , do not show any clear correlation with the coefficient of SS11, either.

In the last column of Table 2 we present characteristic values of the regional SS11 obtained by multiplying the local  $\epsilon$  by the local SW11. Evidently, the SS11 variations between individual regions are quite large - from 1.7 cm in the Arabian Sea to 7.1 cm in the Gulf Stream Extension, and the SSB dependence on wind and wave factors is more complicated than can be described based on simple models like (4) and (6). Figure 3 shows a great diversity of SSB regimes: from a virtual independence of  $\epsilon$  on the pseudo wave age - for the Southern Ocean and the Agulhas Current region, and to a very strong dependence  $\epsilon(\xi)$  - for the Guinea region of the South Atlantic, the Arabian Sea and the North Atlantic. Therefore, the use of SSB models with global coefficients summarized in Table 1 would lead to considerable distortions of sea level in certain regions. The size of these distortions (up to 4 cm) is easy to estimate by differencing these curves from the global GMF. The geographic distribution of SSB based on the GMF (4),(5) with global parameters is illustrated in Fig. 9, and the distribution of the pseudo wave age is given in Fig. 10. The reader is invited to compare SSB values in the regions marked in Fig. 2 with those reported in Table 2.

The SS11 correction based on the global GMF appears to be of reasonable accuracy for coarse-spatial-resolution analysis of ocean dynamics. However, for applications requiring fine resolution, the present GMF models must be improved.

#### 4. Cautionary remarks.

The present statistical technique, section 2, has certain advantages as well as drawbacks. The latter must be kept in mind when comparing the present results with those of other authors. One assumption of the present method is that the SSB as a function of external factors is statistically independent of all other components of the satellite-reported sea level height. Although this assumption is physically well justified for open ocean conditions, it may be violated in (hopefully, a small number of) special cases. For example, within enclosed basins and at small local depths (e.g., the North Sea or coastal areas of the Gulf of Mexico), the mean sea level responds to variations of wind and wave height (i.e., storm surges) rather rapidly. This may yield an appreciable correlation between  $\zeta^{\text{true}}$  and  $\eta$ . Furthermore, uncertainty in some of the corrections used in altimeter data processing, for instance errors in dry troposphere and inverse barometer corrections (both derived from a model-based atmospheric pressure rather than the actual atmospheric pressure), may be (weakly) correlated with the local wind, hence with the factors of SSB. Finally, the orbit correction, being based on a sine function (of the earth-size period) fitted to the sea level for each orbit, may also contain some information about

the global distribution of SSB (provided the spatial variation of SSB along the satellite pass has a non-zero Harlh-period component). This could theoretically introduce a slight filtering effect into the data. All such effects are expected to be insignificant. Nonetheless, they should not be dismissed *a priori*, and their study would be most welcome.

Of much greater importance is the effect of the spatial filtering of the input data. The nine-point median filter reduces the measurement noise, as described in the end of section 4, and is justified if the sea level data are to be used in global ocean studies. Indeed, the resulting (actually, rather slight) smoothing of the data over the distance of about 60 km is consistent with the input requirements for ocean circulation models run on a 1 by 1 degree grid. However, this filtering also suppresses effects of the wind fetch on the sea state bias, which is why the present work yields slightly reduced values of  $\epsilon$  as compared to those of other authors. The optimal constant  $a_0$  for the simplest SSB model,  $\epsilon \equiv a_0 = 0.018$ , found in the present work is slightly smaller than some of the previous estimates. However, the spatial filtering can hardly affect our comparisons of different SSB algorithms, for all of them are affected simultaneously.

The launch of ERS-1 and Topex/Poseidon satellites prompted new activity in the area of SSB modeling. Several techniques used by various research groups, including the technique described in section 2, will eventually yield independent estimates of the accuracy gain by different SSB models as well as of the optimal parameters for SSB models and the models comparisons. Since experimental procedures and criteria for rejection of "bad" data employed by different authors are inevitably different, it is natural to anticipate disagreements in the results. Some of possible discrepancies can be eliminated if a few general rules are followed. We recommend the following. 1) The accuracy gains (or any other quantitative measure of SSB improvement) should be calculated based on global subsets of points uniformly distributed over the World Ocean and not including points used in the derivation of the model parameters. Wind and wave statistics for such test subsets should be derived and reported - to make sure the test data are statistically equivalent to those of other authors. 2) individual measurements affected by known adverse technical characteristics of a satellite instrument should be eliminated from the data sets. For instance, more than a half of all Geosat altimeter measurements had to be eliminated in this work because of a large attitude angle. 3) Since SSB is obtained as a function of altimeter-supplied wind, the use of different wind speed GMI's may also contribute to discrepancies between SSB models. In the present work we used

the wind model [Glazman and Greysukh, 1993] characterized by the smallest mean and rms errors.



## 7. Conclusions

Our analysis of regional SSB variations showed that the actual SSB variability is greater than what would be obtained based on the predictions of the global GMFs. Respectively, the maximum accuracy gain of 2.55 cm reported in Table 1 is probably far below the actual, physically-based limit,

Further progress in SSB modeling can hardly be achieved by increasing the number of terms in polynomial GMFs. Theoretically justified models employing meaningful combinations of external parameters appear to be more promising. The pseudo wave age is one such combination. However, according to both the theory and the present data, this parameter accounts for only a part of the total SSB variability. As an additional relevant parameter, one may try to use the "generalized wind fetch" defined by (15). However, an additional effort is needed to establish its usefulness as a measure of the actual geometric fetch. Possibly, some additional information, for instance wind maps based on satellite scatterometry or/and characteristic lengths of dominant surface gravity waves available from SAR, might be of help.

Practical estimation of SSB based on satellite-supplied data has intrinsic limitations. In particular, wind speed and SWH do not necessarily provide a sufficient set of parameters from which to infer the actual geometrical properties of a random sea surface responsible for SSB. The theory underlying the model (2)-(5) is highly idealized and may be inadequate in certain situations. The present analysis of regional SSB variations, as well as the above mentioned work by other authors, indicate that our understanding of physics mechanisms responsible for SSB is incomplete: we cannot point exactly at all possible causes of SSB variations.

The characteristic values of  $c$  obtained in the present work are slightly below (by about 20 to 30 percent) the values reported in some of the previous Studies. As the most likely cause of this discrepancy we point at the nine-point (60 km) spatial filtering of the data (see sections 4 and 6). However, we emphasize that the filtering can hardly have any effect on our main conclusions regarding the relative performance of individual algorithms, for it affects all the models in the same fashion.

**ACKNOWLEDGMENTS:** This work was performed at the Jet Propulsion Laboratory, California Institute of Technology, under contract with the National Aeronautics and Space Administration.

## REFERENCES

Barrick, D.E. and B.J. Lipa. Analysis and interpretation of altimeter sea echo. Advances in Geophysics, Vol. 27, 60-99, 1985

Born, G.I., M.A. Richards and G.W. Rosborough. An empirical determination of the effects of sea state bias on SEASAT altimetry. J. Geophys. Res., 87(C5), 3221-3226, 1982

Brown, G. S., 1977. The average impulse response of a rough surface and its applications. IEEE Trans. Antennas and Propagat., AP-27, 67-74

Chelton, D.B., E.J. Walsh and J.J. MacArthur. Pulse compression and sea level tracking in satellite altimetry. J. Atm. Oceanic. Technol., 6(3), 407-438, 1989

Cheney, R. E., W.J. Emery, B.J. Haines, and F. Wentz, Recent Improvements in Geosat Altimeter Data. Eos, 72, p 577, 1991

Cheney R.E., B.C. Douglas, R.W. Agreen, L.J. Miller, D.L. Porter, Geosat Altimeter Geophysical Data Record (GDR) User Handbook, NOAA Tech. Memo, NOS-NGS-46, 1987.

Choy, L. W., D.L. Hammond, and E.A. Uliana, Electromagnetic bias of 10-GHz, radar altimeter measurements of MSJ. Mar. Geod., 8, 297-312, 1984

Dennis, J.E. Jr., and R.B. Schnabel, Numerical Methods for Unconstrained Optimization and Nonlinear Equations, Prentice-Hall, Englewood Cliffs, N. J., 1983.

Emery, W. J., G. H. Born, D. G. Baldwin and C. Norris, Satellite Derived Water Vapor Corrections for GEOSAT Altimetry, J. Geophys. Res. 95, 2953:2964, 1990.

Fu, Lee-Lueng and R.E. Glazman, The effect of the degree of wave development on the sea-state bias in radar altimetry measurements. J. Geophys. Res., 96(C1), 829-834, 1991

Glazman, R.E., 1986, Statistical characterization of sea surface geometry for a wave slope field discontinuous in the mean square. *J. Geophys. Res.*, 91 (C5), 6629-6641.

Glazman, R. E., 1987. Wind-fetch dependence of Seasat scatterometer measurements. *Int. J. Rem. Sensing*, 8(1 1), 1641-1647.

Glazman, R.E., G.G. Pihos and J. Ip, 1988. Scatterometer wind-speed bias induced by the large-scale component of the wave field. *J. Geophys. Res.*, 93(C2), 1317-1328.

Glazman, R.E. and A. Greysukh, 1993. Satellite altimeter measurements of surface wind. *J. Geophys. Res.* 98(C2), 2475-2483.

Glazman, R.E., and M.A. Srokosz, Equilibrium wave spectrum and sea state bias in satellite altimetry. *Journ. Phys. Oceanogr.*, 21(11 ), 1609-1621, 1991

Glazman, R. E., and P. Weichman, 1989. Statistical geometry of a small surface patch in a developed sea. *J. Geophys. Res.*, 94(C4), 4998-5010.

Glazman, R.E., and S.11. Pilorz, 1990. Effects of sea maturity on satellite altimeter measurements. *J. Geophys. Res.*, 95(C3), 2857-2870.

Haines, B. J., G.H. Born, G.W. Rosborough, and J.G. Marsh, Precise Geosat Orbits for the Geosat Exact Repeat Mission, *J. Geophys. Res.*, 95(c3), 2857-2870, 1990.

Hayne, G.S., Radar altimeter mean return waveforms from near-normal-incidence ocean surface scattering. *IEEE Trans. Antennas Propagat.*, AP-28, 687-692, 1980

Jackson, F. C., 1979. The reflection of impulses from a nonlinear random sea. *J. Geophys. Res.*, 84(C8), 4939-4943,

“Melville, W.K., R.11, Stewart, W.C. Keller, J.A. Kong, D.V. Arnold, A. J’. Jessup, M.R. Löwen, and A.M. Slinn. Measurements of electromagnetic bias in radar altimetry. *J. Geophys. Res.*, 96(C3), 4915-4924, ] 991

Ray, R.D. and C.J. Koblinsky, On the sea state bias of the Geosat altimeter. *J. Atmos. Oceanic Technol.*, 8,397-408. 1991

Rodriguez, E., Altimetry for non-Gaussian oceans: height biases and estimation of parameters. *J. Geophys. Res.*, **93**(C11), 14107-14120, 1988

Srokosz, M. A., On the joint distribution of surface elevation and slopes for a nonlinear random sea, with an application to radar altimetry. *J. Geophys. Res.*, **91** (C1), 995-1006, 1986.

Walsh, E. J., F.C. Jackson, E.A. Uliana, and R.N. Swift, 1989. Observations on electromagnetic bias in radar altimeter sea surface measurements. *J. Geophys. Res.*, **94**(C10), 14,575-14,584.

Walsh, E. J., F.C. Jackson, D.E. Hines, C. Piazza, L.G. Leivizi, D.J. McLaughlin, R.E. McIntosh, R.N. Swift, J.F. Scott, J.K. Yungel, E.B. Frederick, Frequency dependence of electromagnetic bias in radar altimeter sea surface range measurements. *J. Geophys. Res.*, **96**, C(11), 20,571 -20,583, 1991

Witter D.L. and D.B. Chelton. An apparent wave height dependence in the sea-state bias in Geosat altimeter range measurements. *J. Geophys. Res.*, **96**(C5), 8861-8867, 1991.

Wentz, F. J., User's Manual SSM/I Geophysical Tapes, RSS Tech. Report 060989, Remote Sensing Systems, Santa Rosa, CA, 16pp, 1989

Yaplee, B. S., A. Shapiro, D.J. Hammond, B.B. Au, and E.A. Uliana, 1971. Nanosecond radar observations of the ocean surface from a stable platform, *IEEE Trans. Geosci. Electron.*, **GE-9**, 170-174.

Zlotnicki, V., L.-L. Fu and W. Patzert. Seasonal variability in global sea level observed with Geosat altimetry. *J. Geophys. Res.*, **94**(C12), 17,959-17,969, 1989.

Zlotnicki, V., A. Hayashi and L.-L. Fu, The JPL-Oceans 8902 version of Geosat Altimetry data, JPL Internal Document 11-6939, Jet Propulsion Lab., California Institute of Technology, Pasadena, CA 91109, 1990

Zlotnicki, V., Sea Level Differences across the Gulf Stream and Kuroshio extension, *J. Phys. Oceanog.*, **21** (4), 599-609., 1991

Table 1, Ratings of empirical model functions for SS11 correction.

Model source and version	Type of experiment	Radar band, GHz	Wind-wave factors of & included in equation (#)	Empirical parameters in eqs (6), (7) and (4)			Accuracy gain $\langle(\Delta\eta)^2\rangle^{1/2}$ cm	
				a <sub>0</sub>	a <sub>1</sub>	a <sub>2</sub>		
M [91], (A)	Sea tower radar	14.0	U, II; (6)	.0146	.00215	.00389	loss	
" (B)			$\sigma_0^{-2}$ , II; (7)	<b>.0163</b>	<b>2.15</b>	.00291	loss	
" (C)			U; (6)	<b>.0179</b>	<b>.0025</b>		loss	
W [91], (A)	Airborne radar	13.6	U; (6)	<b>.011</b>	<b>.0014</b>		1.24	
" (B)		5.3	U; (6)	<b>.0074</b>	<b>.0025</b>		N/A	
w [84], (C)		36.0	U; (6)	<b>-.0019</b>	<b>.0012</b>		N/A	
R&K [91]	Geosat altimeter	13.5	U; (6)	<b>.0066</b>	<b>.0015</b>		1.67	
F&G [91]			$\xi$ ; (4)	<b>.027</b>	<b>.88</b>		2.54	
			Optimized (MF's for global Geosat data :					
Constant $\epsilon$			none	<b>0.018</b>				1.94
Linear wind			U; (6)	<b>.0056</b>	<b>.00091</b>			2.25
Linear SWH			II; (6)	<b>.0327</b>		-.0022		2.01
Linear wind and SWH			U, II; (6)	<b>.0245</b>	<b>.00122</b>	-.0034		2.46
Present			$\xi$ ; (4)	<b>.026</b>	<b>.56</b>			2.55

**Notation:**

M[91]: Melville et al. [1991]; W[84] and [91]: Walsh et al. [1984] and [1991]; R&K [91]: Ray and Koblinsky [1991]; F&G [91]: coefficients a<sub>0</sub> and a<sub>1</sub> are to be understood as M and m in eq. (4) for GMF of Fu and Glazman, 1991]; "Linear wind": eq. (6) with a<sub>2</sub>=0 and coefficients a<sub>0</sub> and a<sub>1</sub> optimized as described in section 5. "Linear SWH": eq. (6) with a<sub>1</sub>=0, and a<sub>0</sub> and a<sub>2</sub> optimized as described in section 5. "Linear wind and SWH": eq.(6) with all three coefficients optimized. "Present" : eq. (4) with parameters M and m refined as described in section 5. Blank cells for the values of a<sub>1</sub> and a<sub>2</sub> signify that the corresponding terms are dropped in a given GMF.

**Table 2**

Characteristics and optimal parameters for ocean regions

Region	Mean regional values				total $dZ^2$ variance	Ops = a0	ops = a0 + a1*U		SSB (cm)
	U (m/s)	H (m)	xi	x (m)			a0	a1	
1	5.8	2.1	2.9	2.0	9.9	0.020	0.005	0.0016	4.2
2	6.0	1.3	2.2	0.9	16.6	0.013	0.011	0.0002	1.7
3	5.9	2.1	3.0	2.2	14.0	0.028	-0.004	0.0028	5.8
4	5.2	1.6	2.8	1.5	9.4	0.020	0.002	0.0023	3.2
5	8.6	3.1	2.3	1.9	15.0	0.016	0.005	0.0007	4.9
6	8.8	3.5	2.5	2.8	16.6	0.015	0.014	0.0001	5.2
7	7.6	3.3	2.9	3.2	33.7	0.014	0.021	-0.0005	4.6
8	8.3	2.8	2.2	1.7	31.6	0.026	0.032	-0.0004	7.1
global	7.1	2.6	2.7	2.3	18.8	0.018	0.006	0.0009	4.6

FIGURE CAPTIONS for “Sea state bias in satellite altimetry: ..” by R. Glazman, A. Greysukh and V. Zlotnicki

Figure 1. The total variance  $\langle(\Delta\zeta)^2\rangle$  of surface increments, equation (12), as a function of parameters  $M$  (denoted as  $a_0$ ) and  $m$  (denoted as  $a_1$ ) in the SSB model (4).

Apparently, near its minimum,  $\langle(\Delta\zeta)^2\rangle$  is more sensitive to variations in  $M$  than it is to variations in  $m$ .

Figure 2. Ocean regions selected for the evaluation of sensitivity of the SSB model to regional factors.

Figure 3. SSB coefficient  $c(\xi)$  estimated for individual regions. Numbers at the curves correspond to the regions in Fig. 2.

Figure 4. Estimates of empirical model parameters in (4) for 20 global subsets,

Figure 5. The total variance, equation (12), as a function of parameters  $a_0$  and  $a_1$  in the sea state bias model (6) with  $a_2=0$ .

Figure 6. The total variance, equation (12), as a function of parameters  $a_0$  and  $a_2$  in the sea state bias model (6) with  $a_1=0$ .

Figure 7. The total variance, equation (12), as a function of parameters  $a_1$  and  $a_2$  in the sea state bias model (6) in which  $a_0$  is fixed at its optimal value.

Figure 8. Dependence of the SSB coefficient  $c = a_0$  obtained for each individual region on the significant wave height,  $H$ , (upper pannel) and the "generalized wind fetch",  $X$ , (lower pannel), characteristic to these regions. Numbers indicate regions shown in Fig. 2.

Figure 9. Global distribution of SSB calculated based on (12) and (4) for the 2.5 year period of Geosat altimeter data.

Figure 10. Global distribution of the pseudo wave age,  $\xi$ , for the 2.5 year period of Geosat altimeter data.

a 1

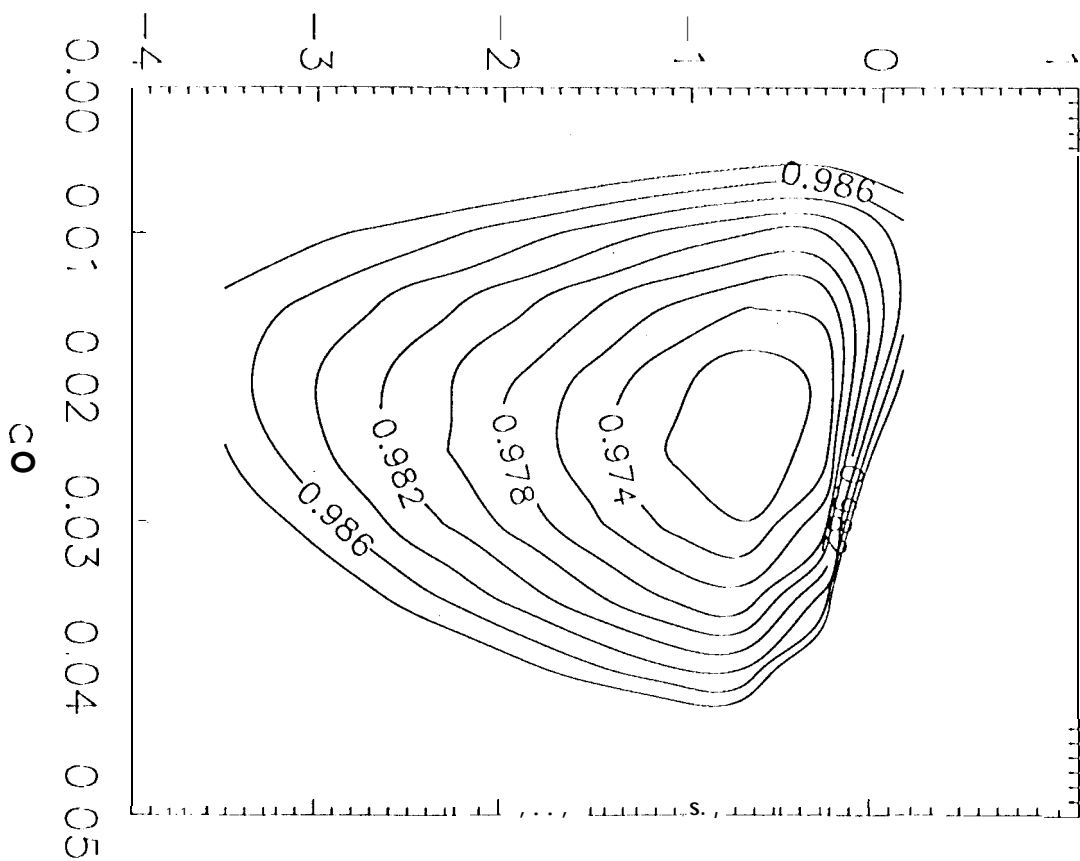
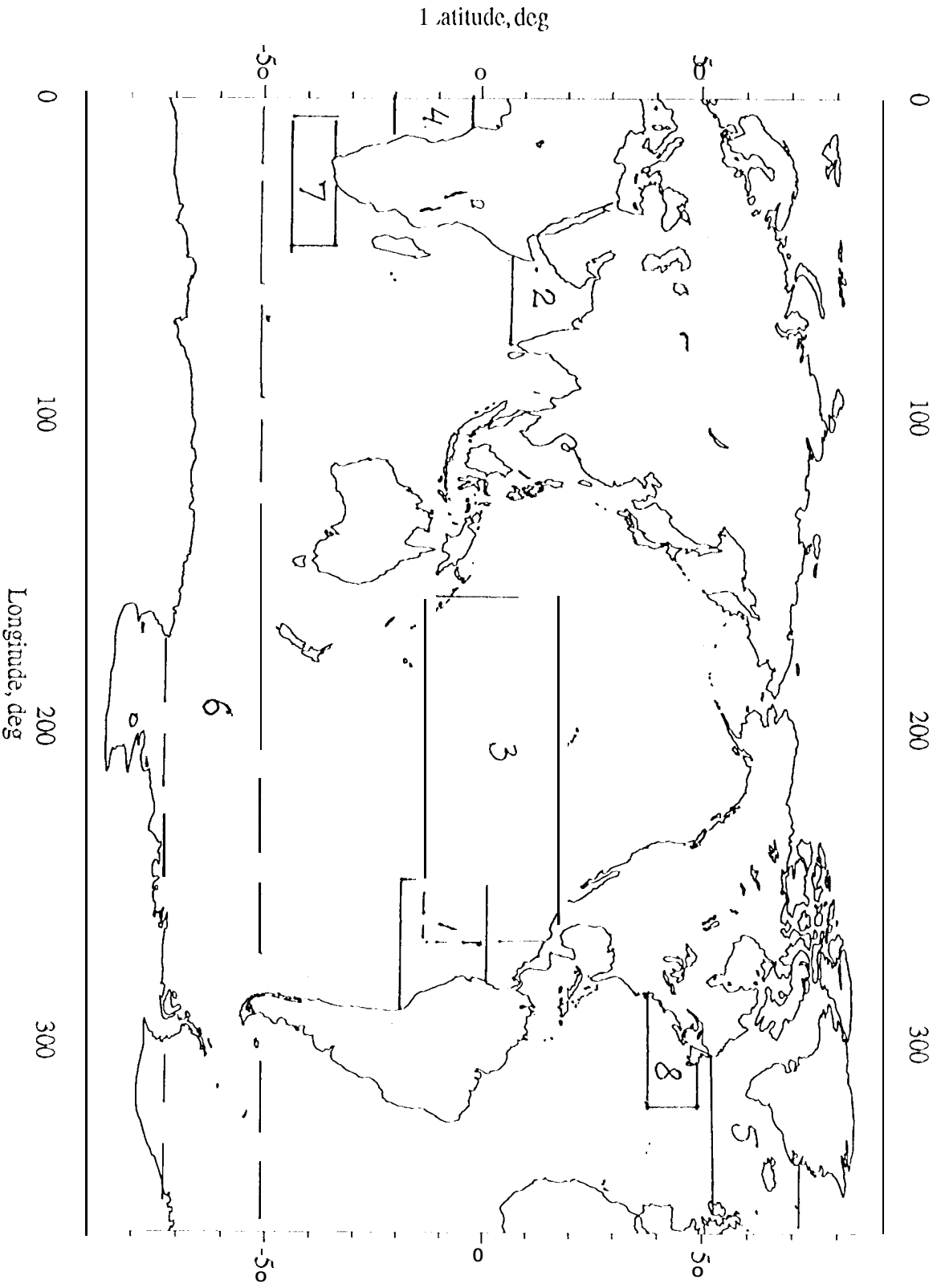
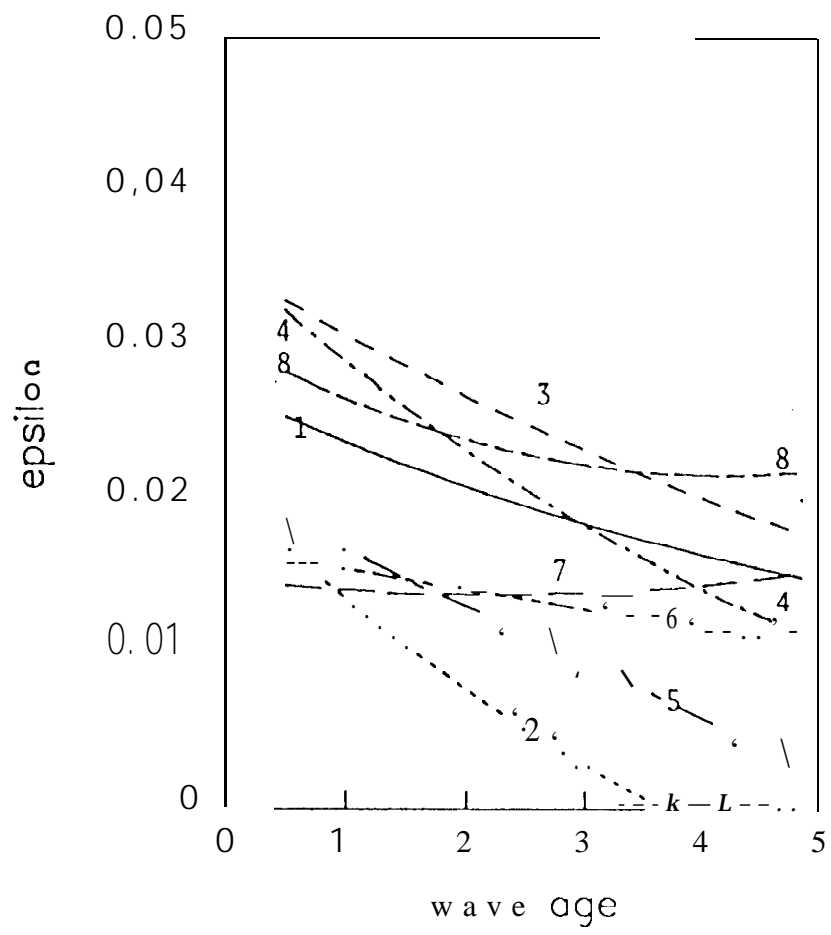


Fig 1







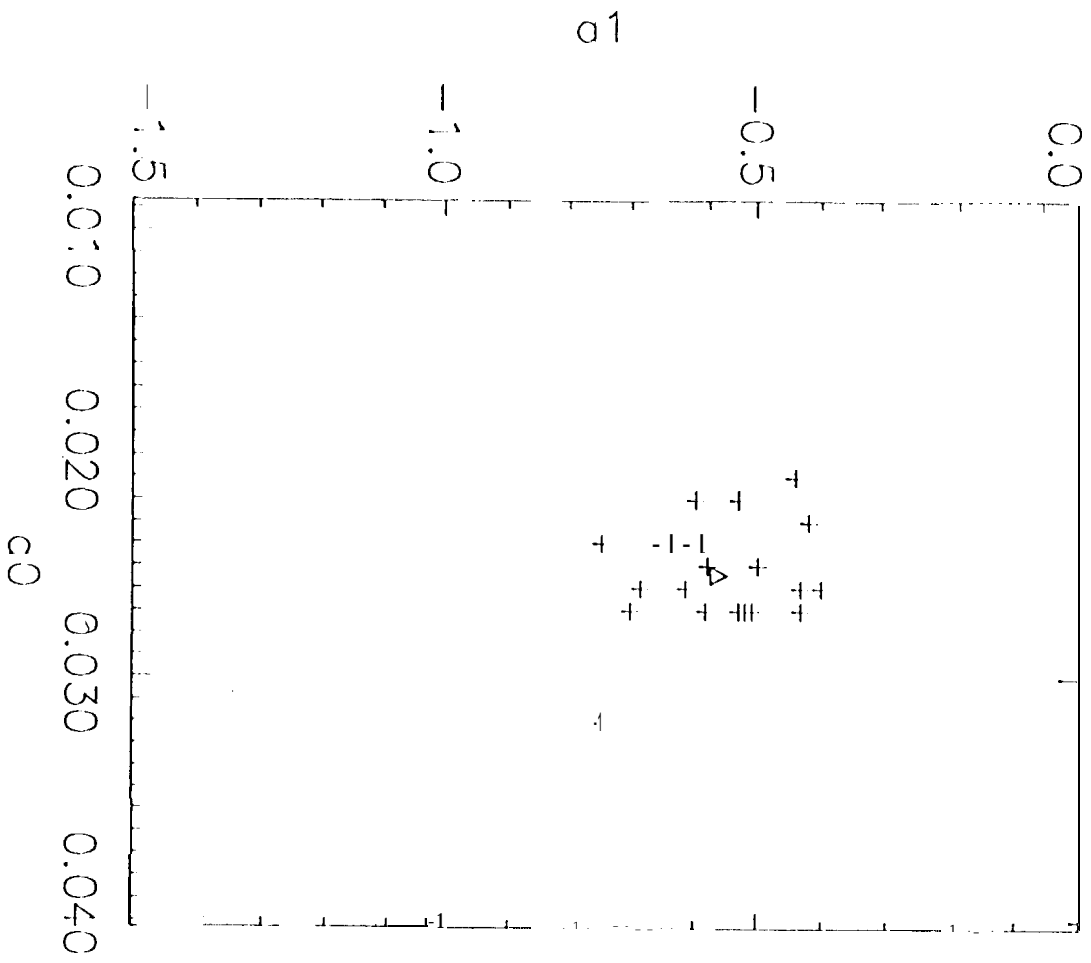


Fig. 5

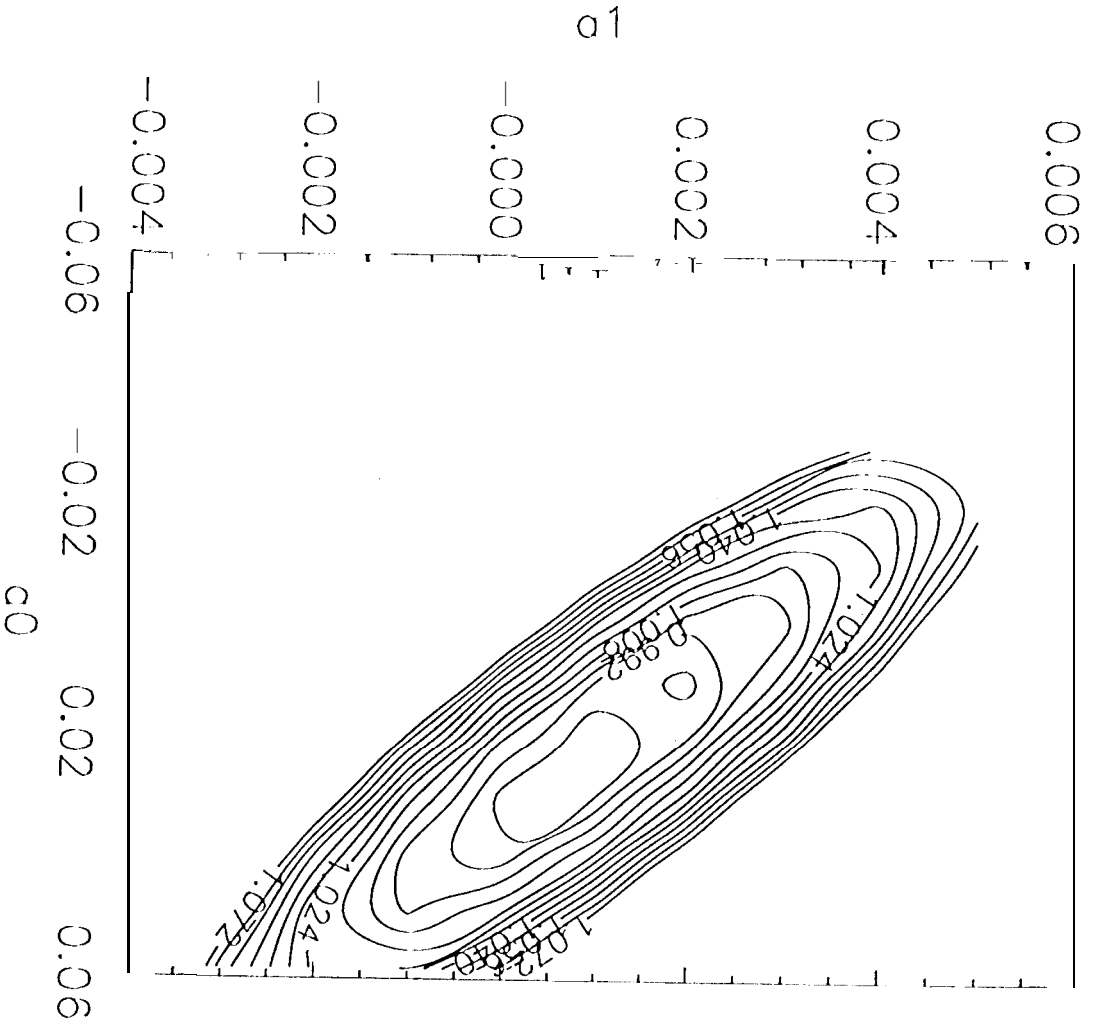


Fig. 5

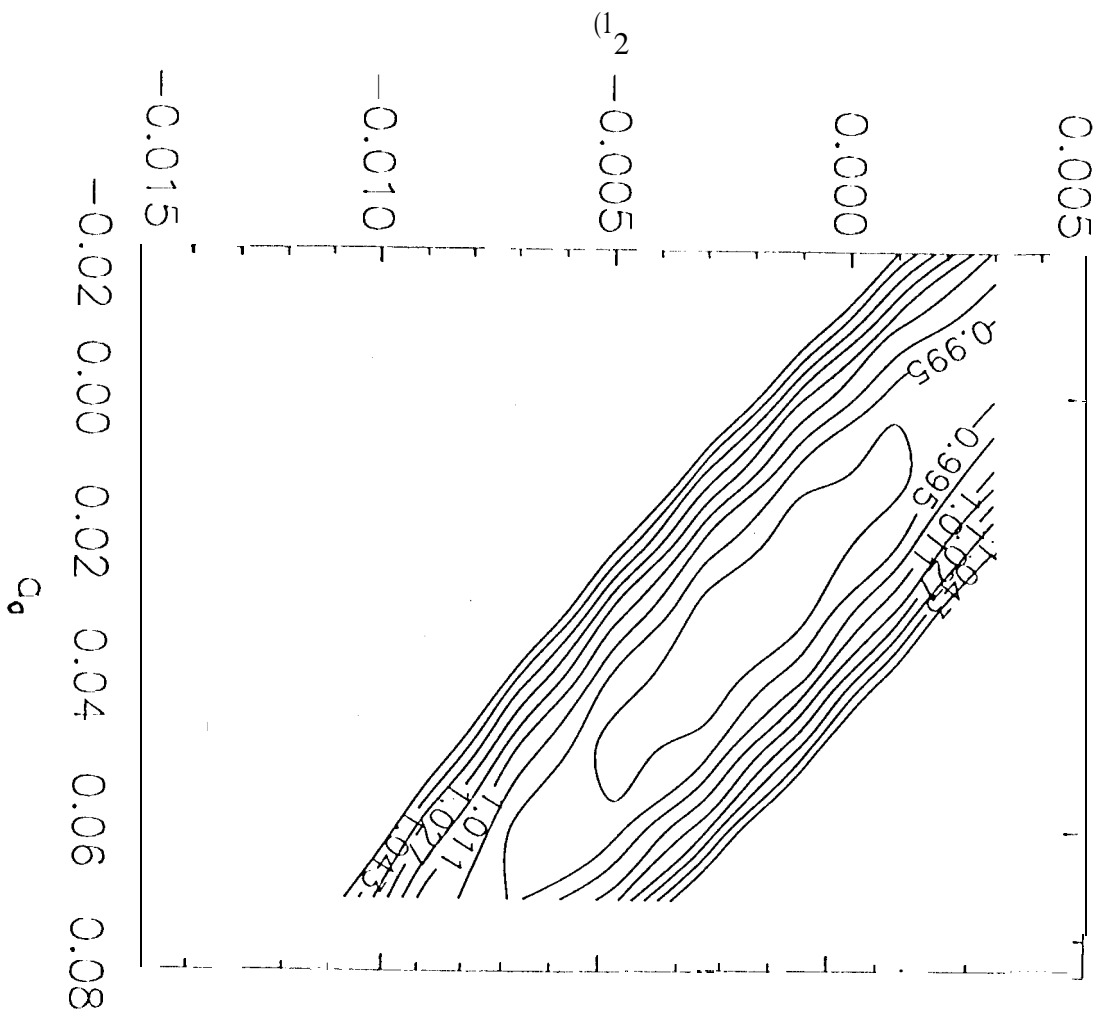
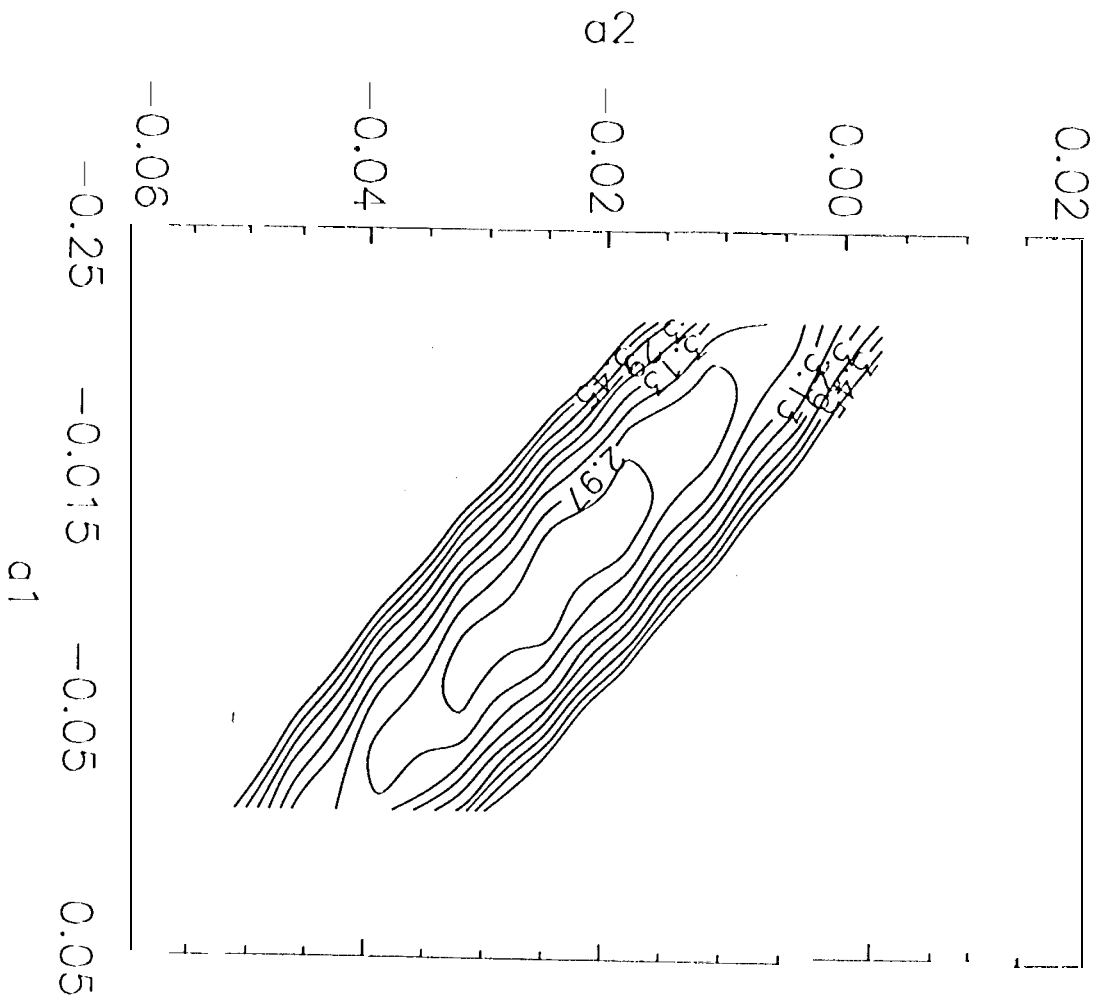
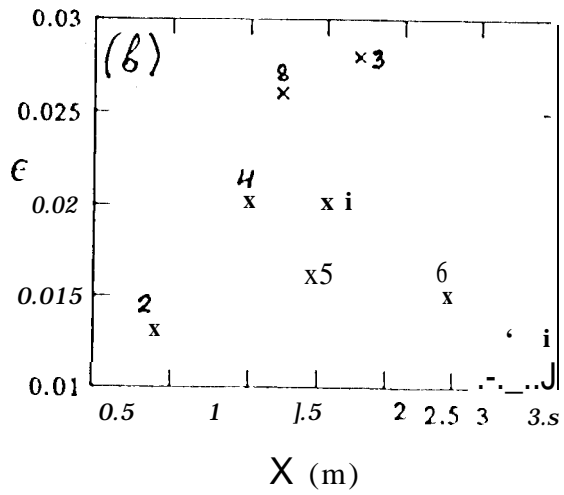
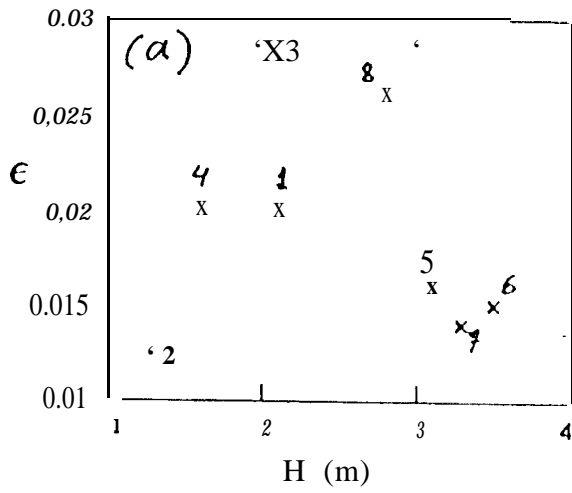


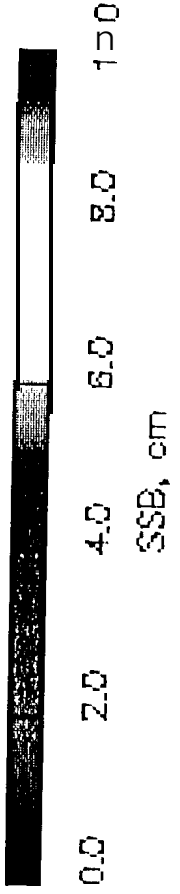
Fig. 6



10

13/11









1.0 2.0 3.0 4.0 5.0 6.0  
pseudo wave age